IC/91/112

INTERNATIONAL CENTRE FOR THEORETICAL PHYSICS

NONSTANDARD FAREY SEQUENCES IN A REALISTIC DIODE MAP

Gabriel Perez

Sudeshna Sinha

and

Hilda Cerdeira

INTERNATIONAL ATOMIC ENERGY AGENCY

UNITED NATIONS EDUCATIONAL, SCIENTIFIC AND CULTURAL ORGANIZATION

1991 MIRAMARE - TRIESTE

IC/91/112

International Atomic Energy Agency
and
United Nations Educational Scientific and Cultural Organization
INTERNATIONAL CENTRE FOR THEORETICAL PHYSICS

NONSTANDARD FAREY SEQUENCES IN A REALISTIC DIODE MAP

Gabriel Perez, Sudeshna Sinha and Hilda Cerdeira *
International Centre for Theoretical Physics, Trieste, Italy.

ABSTRACT

We study a realistic coupled map system, modelling an $p-i-n$ diode structure. As we vary the parameter corresponding to the (scaled) external potential in the model, the dynamics goes through a flip bifurcation and then a Hopf bifurcation, and as the parameter is increased further, we find evidence of a sequence of mode locked windows embedded in the quasiperiodic motion, with periodic attractors whose winding numbers $\rho = p/q$, are given by a Farey series. The interesting thing about this Farey sequence is that it is generated between two parent attractors with $\rho = 2/7$ and $2/8$, where $2/8$ implies *two distinct coexisting* attractors with $\rho = 1/4$, and the correct series is obtained only when we use parent winding number $2/8$ and not $1/4$. So unlike a regular Farey tree, p and q need not be relatively prime here, $\rho = \frac{2\times p}{2\times q}$ is permissible, where such attractors are actually comprised of two coexisting attractors with $\rho = p/q$. We also checked that the positions and widths of these windows exhibit well defined power law scaling. When the potential is increased further, the Farey windows still provide a "skeleton" for the dynamics, and within each window there is a host of other interesting dynamical features, including multiple forward and reverse Feigenbaum trees.

MIRAMARE – TRIESTE

June 1991

* Also at Instituto de Fisica, Universidade Estadual de Campinas, 13801 Campinas, SP, Brazil.
Associate Member of the INFN (Istituto Nazionale di Fisica Nucleare).

Coupled maps (CM), as models of many component nonlinear physical, chemical and biological systems, have been the focus of much research interest. For instance, realistic models of convection in conducting fluids, *ac*-driven *dc* SQUIDS, instabilities in solids, neurodynamics and polyatomic molecules interacting with strong IR radiation fields such as CO_2 lasers, involve coupled oscillatory processes[1-9]. Extensive studies have mostly been devoted to systems of coupled logistic maps. Here we study a very different kind of coupled map, and elucidate the features of its dynamics.

We consider here a coupled map which describes an interesting physical problem[9], namely a device with a $p-i-n$ diode structure, consisting of two oppositely doped silicon regions separated by a layer of intrinsic silicon. When the $p-i-n$ diode is reverse biased the two regions of fixed charges are separated by their relatively long intrinsic Si region, which acts as an insulator. The $p-i-n$ diode under consideration is kept at low temperature, with a reverse bias voltage $V_0+V(t)$, where $V(t)$ is in synchronysm with the mechanism that produces the change in the density of carriers. The peaks of $V(t)$ make the field at both junctions slightly above the "critical value" for an avalanche process to develop. So a slight change in the density of carriers will trigger an avalanche. During the lower half cycle of $V(t)$ the field is subcritical, stopping the avalanche and sweeping away the electron and hole charge clouds. Such a device will produce a current with an

oscillating component in the following way: a carrier crossing, say, the left junction will produce two charge clouds, one of which moves to the right. As it reaches the second junction it will produce two charge clouds, one of them moving towards the left, and so on. This will produce an oscillation in the current, whose frequency will depend on the distance between the junctions, and should be much higher than the bias voltage.

We consider here a simplified one dimensional structure, with two slabs (representing the junctions), with an electric field applied to them, strong enough to produce an avalanche, separated by a region where the field is weak enough so that particles just drift with a constant velocity (the intrinsic region). Since the behaviour of the density of carriers at a certain slab end depends linearly on the density of carriers of opposite sign at the slab end where it bounced before, we may represent these successive densities as the coupled map[9]:

$$\begin{aligned} x_{n+1} &= c\, y_n \exp\frac{-1}{|V - x_n|} \\ y_{n+1} &= c\, x_{n+1} \exp\frac{-1}{|V - y_n|} \end{aligned} \tag{1}$$

where x and y are the (scaled) densities of the negative and positive carriers respectively, V is the (scaled) potential applied across the junction and c is a parameter associated with the characteristics of the sample whose particular dependence is not of interest here. The discrete time variable n represents successive "bounces" of clouds of charge. The important physical

feature of this system, very different from the usual well known unimodal maps, is the *exponential* in Eq. 1, which is typical of the density of a cloud of charge leaving a junction where a voltage is applied.

We investigate the features of the dynamics as a function of the (scaled) voltage V, as clearly, it is the parameter we can control externally. Fig. 1 shows the bifurcation diagram for V and it is evident that the variation of this parameter gives rise to a very rich and interesting repertoire of phenomena. The dynamics starts with a fixed point behaviour. The fixed points of the map are $x^* = y^* = 0.0$ and $x^* = y^* = V - 1/\log c$. The Jacobian is given by

$$J = \begin{vmatrix} \frac{x_{n+1}\mathrm{sign}(x_n - V)}{(V - x_n)^2} & \frac{x_{n+1}}{y_n} \\ \frac{y_{n+1}\mathrm{sign}(x_n - V)}{(V - x_n)^2} & \frac{y_{n+1}}{y_n} + \frac{y_{n+1}\mathrm{sign}(y_n - V)}{(V - x_n)^2} \end{vmatrix} \tag{2}$$

At a fixed point J becomes

$$J = \begin{vmatrix} q & 1 \\ q & 1 + q \end{vmatrix} \tag{3}$$

where $q = x^*/(V - x^*)^2$. The absolute values of the eigenvalues of J then are, 0 and 1, for $x^* = y^* = 0$, and so the stability of this fixed point is always marginal[10]. The eigenvalues for the fixed point $x^* = y^* = V - 1/\log c$, are

$$\lambda = \log c|1 - V \log c| + 1/2 \pm \sqrt{\log c|1 \quad V \log c| + 1/4}.$$

This implies that the stability of this fixed point is dependent on the value of V, for fixed c. It is easy to see that at V just greater than $1/\log c$ the

absolute value of both the above eigenvalues become smaller than 1, and there is an exchange of stability, or the so-called flip bifurcation[11]. So the fixed point $x^* = y^* = V - 1/\log c$ gains stability. This fixed point retains stability until the absolute value of one of the λ's exceed 1. The system then undergoes a Hopf bifurcation, giving rise to radial attractors. In this work, we set the value of $c = 6.5$. For this value of c the two bifurcations occur at $V = 0.534244$ and $V = 0.819661$.

It was observed that the stable phase space attractors associated with various values of V after the Hopf bifurcation are one dimensional curves (see Fig. 2), with the unstable fixed point $x^* = y^* = V - 1/\log c$ as the approximate "center". This diode map then effectively behaves as a "circle" map[12], and can be well described by an angle variable $\Theta = \tan^{-1}(y - y^*)/(x - x^*)$. So this system can be considered as a very *non standard example of a circle map arising from a realistic model of a device.*

Note here that the parameters of this system are related to the well known parameters of the general circle map, Ω and K, in a non obvious fashion. In fact the tuning of the external potential V, which in this case is the relevant parameter to be controlled in the experimental context, would effectively imply traversing the $\Omega - K$ space of a conventional circle map, in an oblique curve. So, it becomes of importance to find through numerical experiments, the phenomenology of this map with respect to changing V, in

order to be able to make contact with experiments. In particular, we would also like to check phenomenologically what Farey sequences we encounter (if any) and whether scaling holds, while we cut across the Arnold tongues in a complicated curve[13].

We find, that in the segment of parameter space, $V \sim 0.89 - 0.92$, there are several periodic windows, supporting attractors with Farey tree properties[13]. The first such, rather wide, window supports an attractor with winding number, $\rho = 2/7$. Between the Hopf bifurcation and this 7 window, only quasiperiodic motion is evident, characterised by limit cycles (continuous 1- dimensional curves in phase space) whose largest Lyapunov exponents are zero. After the 7 window there is another wide window with 8 lines. The interesting thing about this 8 window is that it is actually comprised of *two distinct coexisting attractors*, each with periodicity 4 and $\rho = 1/4$. In the $\Theta - V$ space the two attractors making up the 8 window appear intercalated. Between these 7 and 8 windows we find a series of narrower windows whose winding numbers are given by a Farey tree generated between 2/7 and 2/8. The significant feature to note here is this: the correct sequence of winding numbers is *not* generated by the parent winding number 1/4, but we must use 2/8 as the parent in generating the tree. So the coexistence of attractors must be taken into account in the process of constructing the Farey sequence. This brings us to an important

distinction between this Farey tree and a regular Farey tree. *Here p and q need not be relatively prime, and* $\rho = \frac{2\times p}{2\times q}$ *is permissible.* Whenever we have such a winding number, the window actually supports two coexisting attractors, each with $\rho = p/q$.

The 4/15 window between the basic 2/7 and 2/8 windows is easily seen, and on closer examination we can find the 6/23 window between the 4/15 and 2/8 windows, and the 6/22 window (which implies two attractors with $\rho = 3/11$) between the 4/15 and 2/7 windows, and so on. We have located windows over several generations. Fig. 3 shows a series of them, and Fig. 4 shows the 4/15 window in closer view.

The relevant Farey tree is exhibited in the following table, for the first 3 generations:

2/7							2/8
			4/15				
		6/22				6/23	
	8/29		10/37		10/38		8/31

It is useful to consider sub sets of these windows as "families", whose members are generated by a running index. For instance, the set of windows with winding numbers equal to $\frac{2n}{7+8(n-1)}$, whose continued fraction representation is $(3, 1, 2n-1)$, can be considered to be a family with running index n. This family will then have as members windows with number of lines equal to $7 + 8 \times 1 = 15$, $7 + 8 \times 2 = 23$, $7 + 8 \times 3 = 31$, and so on. The family will accumulate as $n \to \infty$ at the 8 window. Similarly one

can think of families which accumulate at the 7 window, for instance those with winding numbers equal to $\frac{2n}{8+7(n-1)}$.

We expect the positions of windows of a certain family, accumulating, say, at the 8 window, to obey the following scaling form:

$$d_n = d_0\, n^{-\alpha} \tag{4}$$

where the running index is n, and d_0 is a proportionality constant whose value depends on the particular family considered, and d_n is the distance of the nth window of the family[14] from the parent window where this series accumulates as $n \to \infty$. Note here that different families accumulating at a certain window, are intercalated in a regular fashion. For instance, windows with number of lines equal to $7 \times 2 + 8 \times (2n+1)$ always occur between windows with number of lines equal to $7 + 8 \times n$. More specifically, a $14 + 8(2n+1)$ window always occurs between windows $7 + 8n$ and $7 + 8(n+1)$, where $n = 0, 1, 2....$ Now if the different families accumulating at a certain window scaled differently then there would be mis-matches in the intercalation. Since such mis-matches are not seen to occur, we expect α to be independent of the families, as has indeed been observed.

Of course, we have families, that accumulate at the 7 window, and these should also display similar scaling, but with possibly a different exponent and will be given by

$$d_n \quad d_0\, n^{\ \beta} \tag{5}$$

where distance d_n is the distance of the nth window of the family from d_∞ (that is, practically speaking, its distance from the 7 window).

The scaling was verified through numerical experiments over several generations. For numerical convenience, we have concentrated on families accumulating at the 8 window. Fig. 5 shows d_n vs n for the family, with $\rho = \frac{2n}{7+8(n-1)}$. It is clear that scaling holds very well, and the exponent $\alpha = 1.68 \pm 0.01$.

We also checked that the widths of the windows scaled with the number of lines in the window, as a power law, given by

$$w_n = w_0\, n^{-\gamma} \tag{6}$$

where w_0 is a constant whose value depends on the particular family considered, and w_n is the width of the nth window of the family. Fig. 5 shows this power law dependence of the widths of the windows, for the family with winding number equal to $\frac{2n}{7+8(n-1)}$. We find that the value of γ is 2.70 ± 0.01, that is, $\gamma \approx \alpha + 1$. The families accumulating at the 7 window, show faster scaling down of widths, which make them much more difficult to locate as they are extremely narrow[15].

The complicated dynamics following this region has one wide window which supports an attractor with winding number 2/9. Now the 9 window has the additional complexity that each of the 9 branches of the attractor

undergo saddle node bifurcation and we have a region of co-existing 9 attractors. These later disappear and simultaneously another set of 9 lines appear which undergo a Fiegenbaum period doubling cascade, leading to chaos. Further, between the 2/8 and 2/9 windows, a 4/17 window can be seen, and between the 4/17 and 2/8 windows, a 6/25 window. Of course, in these regions of parameter space, the windows provide only a "skeleton" for the system, and there are many very complicated dynamical features, within the windows themselves (see Fig. 6). Most of these additional features (if not all) are Feigenbaum trees, manifested as numerous forward and reverse pitchfork bifurcations (see Fig. 7). This further ties up with the picture that the coupled map we have here is an effective circle map, and tuning parameter V is similar to crossing the $\Omega - K$ space of a conventional circle map, in a complicated curve.

In summary, we have studied the dynamics of a coupled map system describing a realistic $p-i-n$ device, with respect to changing the external potential, which is the relevant parameter from the experimental point of view. The system undergoes a Flip bifurcation and then a Hopf bifurcation, after which it behaves effectively as a "circle" map, displaying a Farey sequence of attractors characterised by clearly evident power law scaling properties. The remarkable thing about this Farey sequence is that it is generated between two periodic windows with winding numbers equal to

2/7 and 2/8, where the 2/8 arises from *two distinct coexisting attractors with winding numbers equal to 1/4*. So $\rho = \frac{2\times p}{2\times q}$ is permissible, and whenever we have such a winding number the window supports two coexisting attractors, each with $\rho = p/q$. As the potential is increased further, the Farey windows still provide the "skeleton" of the dynamics, but within the windows numerous forward and reverse bifurcations can be seen. So tuning the potential is effectively similar to traversing the $\Omega - K$ space of a standard circle map in a very complex curve. This system, then, is an interesting (and non standard) example of a circle map, arising in a non obvious way from a realistic physical model, which has the scope of being checked out experimentally.

Acknowledgements

We are grateful to the Condensed Matter Group at the International Centre for Theoretical Physics, for hospitality.

1. T.A. Hogg and B.A. Huberman, Phys. Rev. **A 29**, 275 (1984)

2. A. Libchaber and S. Fauve, in *Melting, Localization and Chaos*, edited by R.K. Kalia and P. Vashishta (North Holland, New York, 1982)

3. K. Kaneko, Phys. Rev. Lett. **65**, 1391 (1990); G. Perez, S. Sinha and H.A. Cerdeira, submitted to Physica D

4. A. Ferretti and N.K. Rahman, Chem. Phys. Lett. **140**, 71 (1987)

5. L. Glass and M.C. Mackey, *From Clock to Chaos*, (Princeton University Press, Princeton, 1988)

6. *Chaos*, edited by A.V. Holden (Manchester University Press, 1986)

7. W. Freeman, Brain Res. Rev., **11**, 259 (1986)

8. A. Kittel, W. Clauss, U. Ran, J. Parisi, J. Peinke and R.P. Huebner, *20th International Conference in Semiconductors*, Greece, 1990

9. H.A. Cerdeira, A.A. Colavita and T.P. Eggarter, to appear in *Applied Chaos*, edited by J.H. Kim and J. Stringer (John Wiley and Sons)

10. Note that these marginally stable points, $x = y = 0$, sometime appear in the simulations (see Fig. 1 and 6).

11. A.J. Lichtenberg and M.A. Lieberman, *Regular and Stochastic Motion*, Springer-Verlag, New York (1983)

12. M.J. Feigenbaum, L.P. Kadanoff and S.J. Shenker, Physica D **5**, 370 (1982); S. Ostlund, D. Rand, J. Sethna and E. Siggia, Physica D **8**, 303 (1983)

13. M.H. Jensen, T. Bohr and P. Bak, Phys. Rev. A **30**, 960 (984); S. Ostlund and S. Kim, Physica Scripta **T9**, 193 (984); P. Cvitanovic, B. Shraiman and B. Soderberg, Physica Scripta **32**, 263 (1985); S. Kim and S. Ostlund, Physica D **39**, 365 (1989); R. Ecke, J.D. Farmer and D.K. Umberger, Nonlinearity **2**, 175 (1989)

14. Here we measure distance from the centre of the window. The scaling properties however are not crucially dependent on the manner in which d_n is measured, and distances measured from the edge of the windows give quite the same result. This is, of course, understandable, as the windows are very narrow, especially for high n, and distances measured either way give very similar numbers.

15. This makes it much more difficult to obtain the value of β accurately. Preliminary examination (with 5 data points) shows that scaling holds and the value of $\beta \sim \alpha$.

FIGURE CAPTIONS

1. Bifuraction diagram as a function of voltage V, at $c = 6.5$. 100 random initial conditions, chosen from the range $x \in [0.05 : 0.75]$ and $y \in [0.1 : 0.8]$, are plotted here.

2. Stable attractors in phase space ($x - y$ plane) for different values of V, after the Hopf bifurcation ($c = 6.5$).

3. Bifurcation diagram of the region of parameter space between the two basic 2/7 and 2/8 windows, showing the series of narrower windows whose winding numbers are given by a Farey sequence.

4. Closer view of the 4/15 window.

5. Plot of ΔV vs n for the family with winding number equal to $\frac{2n}{7+8(n-1)}$ (this family consists of windows with number of lines equal to: $7 + 8 \times 1 = 15$, $7 + 8 \times 2 = 23$, and so on) for a) $\Delta V = d_n$, the distance of the nth window from the 8 window. b) $\Delta V = w_n$, width of the nth window.

6. Bifurcation diagram of the region of parameter space beyond the 2/8 window, showing the 2/9 window with saddle node bifurcations.

7. Forward and reverse period doubling cascades within the Farey windows.

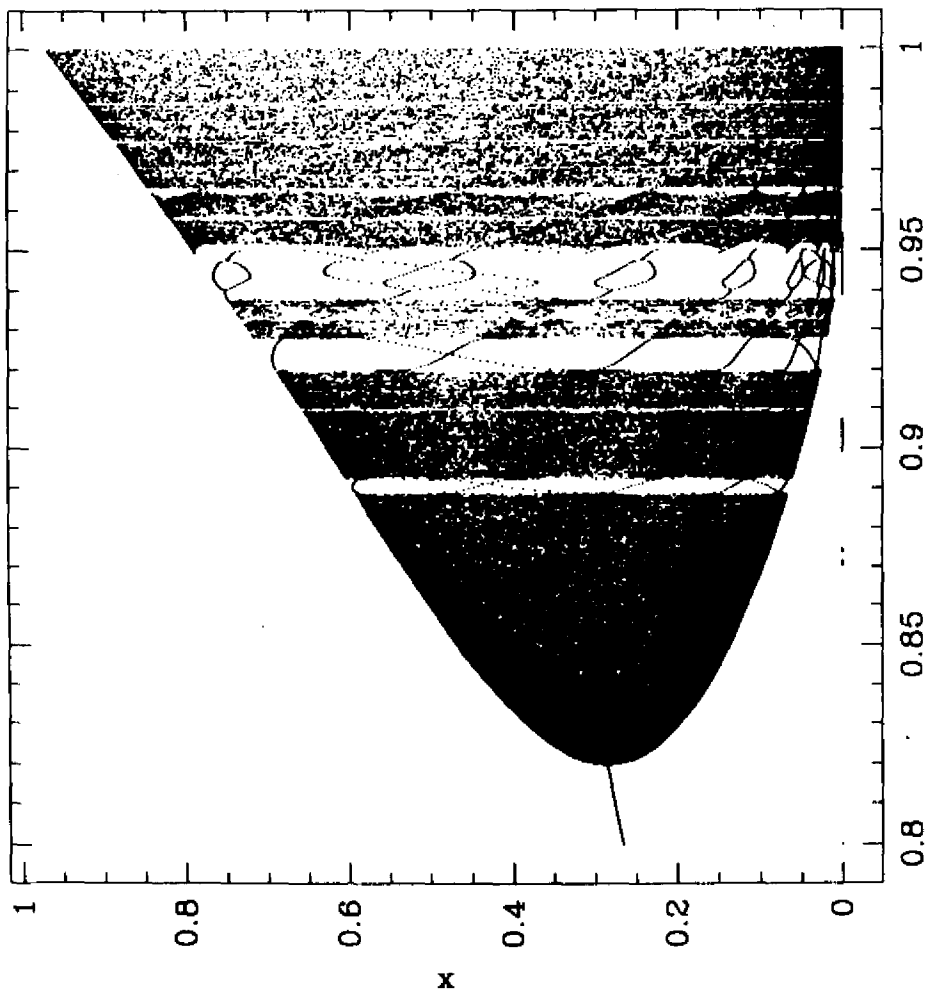

Fig.1

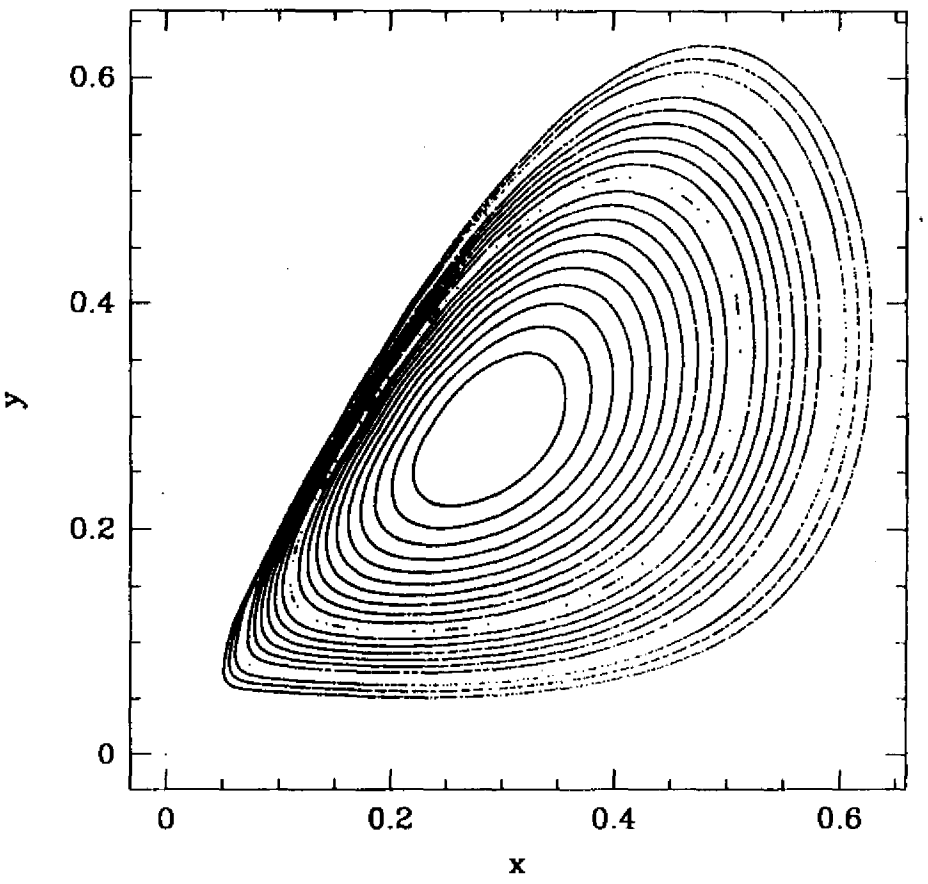

Fig.2

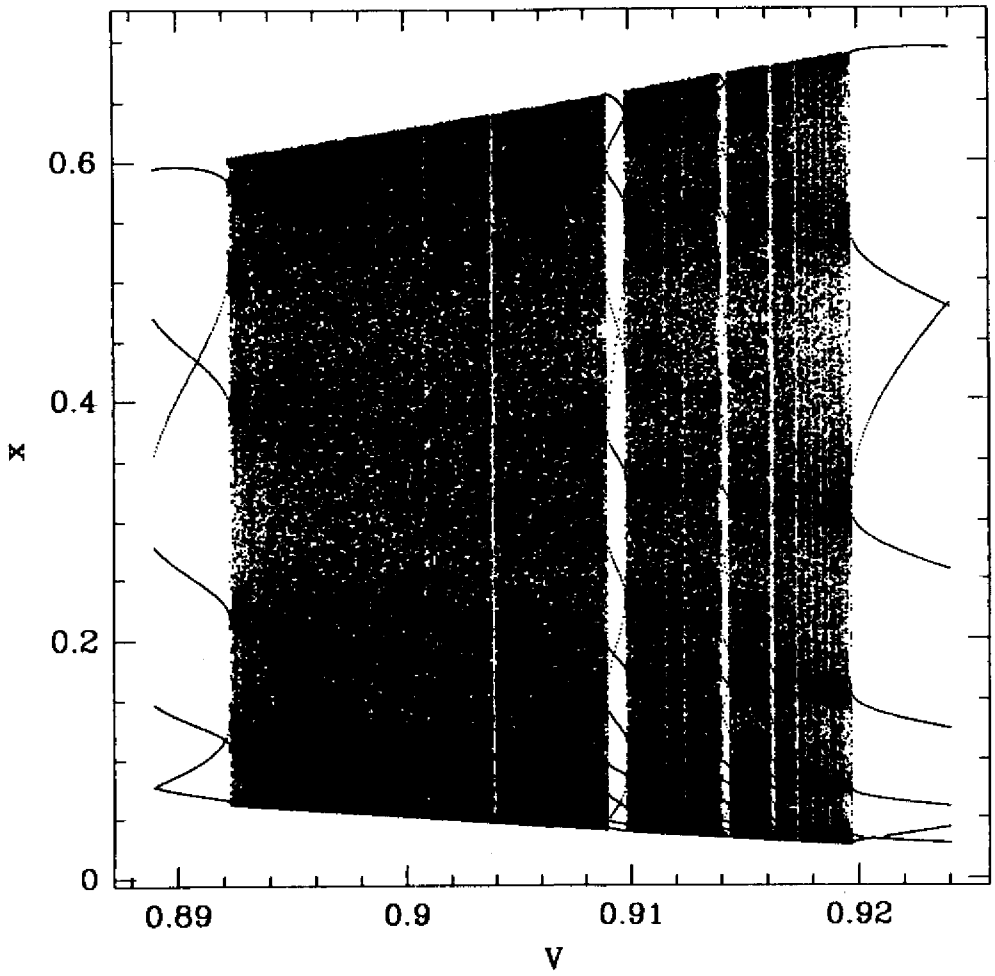

Fig.3

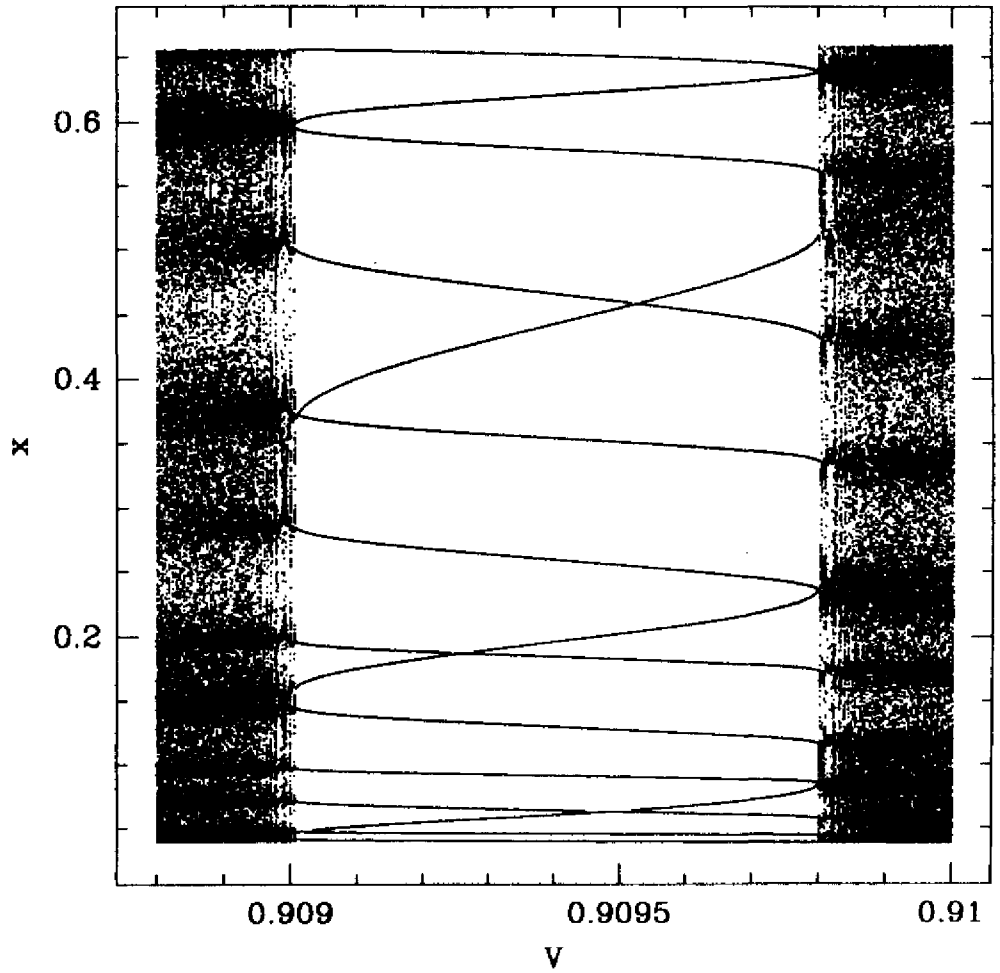

Fig.4

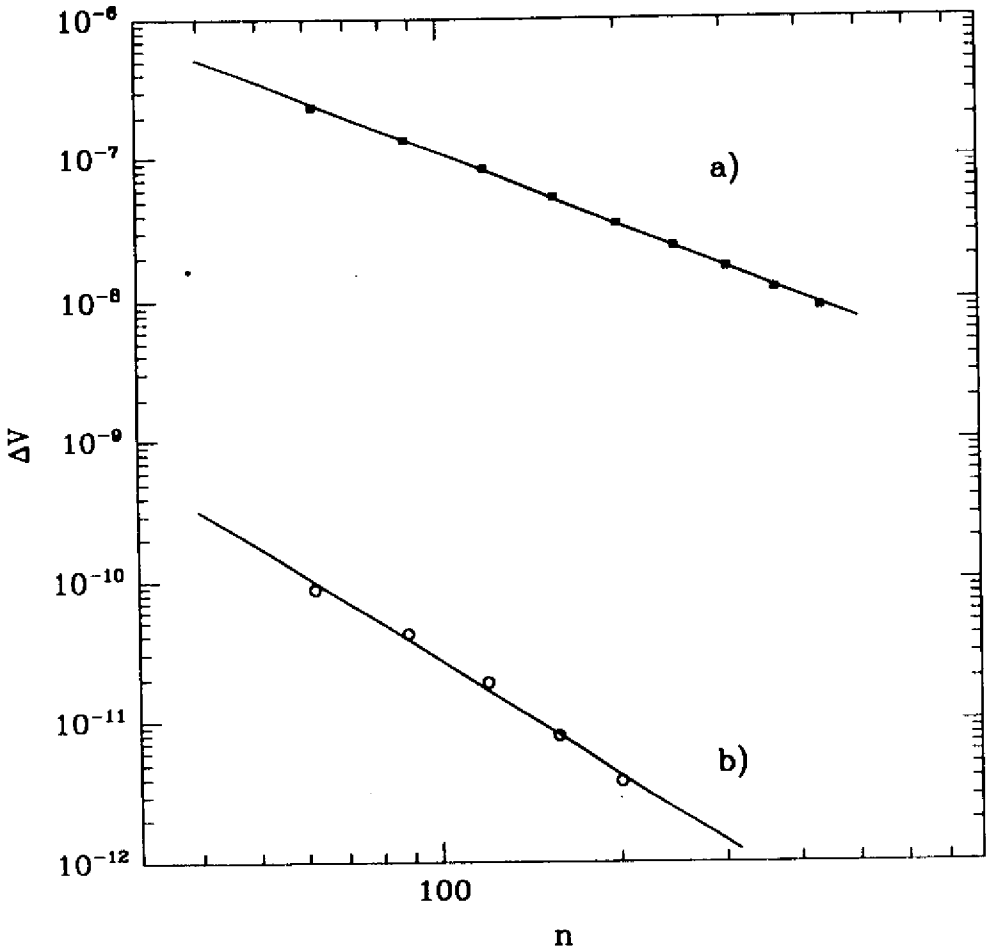
10^{-6}
10^{-7}
10^{-8}
10^{-9}
10^{-10}
10^{-11}
10^{-12}
ΔV
a)
b)
100
n

Fig.6

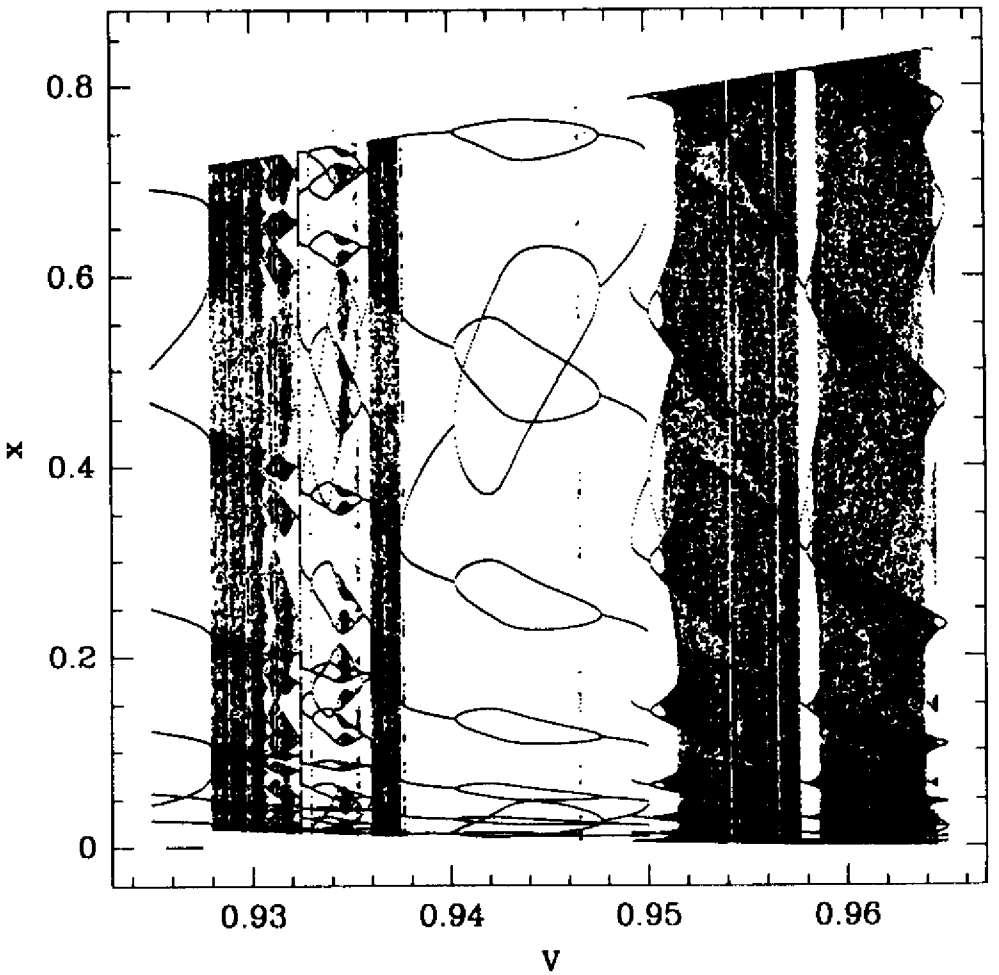
0.8
0.6
0.4
0.2
0
x
0.93
0.94
0.95
0.96
V

Fig.6

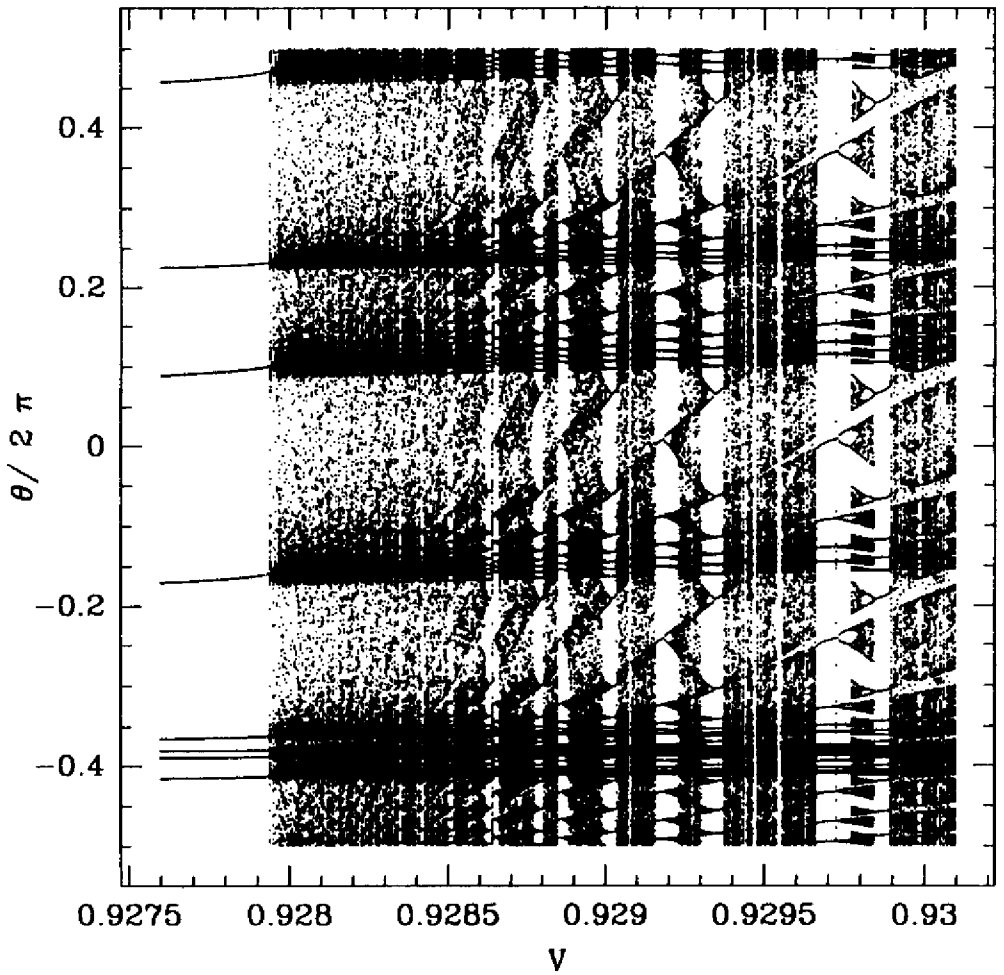

Fig.7